Smart Mater. Struct. **17** (2008) 015013 (12pp) doi:10.1088/0964-1726/17/01/015013

Experimental design and analysis for piezoelectric circular actuators in flow control applications

Poorna Mane[1], **Karla Mossi**[1,3] **and Robert Bryant**[2]

[1] Virginia Commonwealth University, 601 West Main St, Box 843015, Richmond, VA 23284, USA
[2] NASA Langley Research Center, 6 West Taylor St, B1293A, Mail Stop 226, Hampton, VA 23681, USA

Received 11 August 2007, in final form 10 October 2007
Published 3 December 2007
Online at stacks.iop.org/SMS/17/015013

Abstract

Flow control can lead to saving millions of dollars in fuel costs each year by making an aircraft more efficient. Synthetic jets, a device for active flow control, operate by introducing small amounts of energy locally to achieve non-local changes in the flow field with large performance gains. These devices consist of a cavity with an oscillating diaphragm that divides it into active and passive sides. The active side has a small opening where a jet is formed, while the passive side does not directly participate in the fluidic jet. Over the years, research has shown that synthetic jet behavior is dependent on the active diaphragm and the cavity design; hence, the focus of this work. The performance of the synthetic jet is studied under various factors related to the diaphragm and the cavity geometry. Three diaphragms, manufactured from piezoelectric composites, were selected for this study: Bimorph, Thunder® and Lipca. The overall factors considered are the driving signals, voltage, frequency, cavity height, orifice size, and passive cavity pressure. Using the average maximum jet velocity as the response variable, these factors are individually studied for each actuator, and statistical analysis tools are used to select the relevant factors in the response variable. The factors are divided into two experimental fractional factorial design matrices, with five and four factors, respectively. Both experiments are chosen to be of resolution V, where main factors are confounded with three-factor interactions. In the first experimental design, the results show that frequency is not a significant factor, while waveform is significant for all the actuators. In addition, the magnitude of the regression coefficients suggests that a model that includes the diaphragm as a factor may be possible. These results are valid within the ranges tested, that is low frequencies and sawtooth and sine waveform as driving signals. In the second experimental design, cavity dimensions are kept constant and four factors including back pressure are considered. In this case, each diaphragm produces different results with only one diaphragm, Thunder, showing a definite relationship between the studied factors. The other two diaphragms do not show conclusive results, indicating that there may be other factors that need to be considered when pressure is a concern. In summary, independently of the diaphragm utilized in a synthetic jet actuator, applied waveform is an important factor when maximizing peak jet velocity. In addition, frequency is found not to be significant in all cases within the limits of the study. This indicates that the diaphragm and the driving signal should be included in any optimization design of a piezoelectric synthetic jet actuator.

(Some figures in this article are in colour only in the electronic version)

[3] Author to whom any correspondence should be addressed.

1. Introduction

Methods that attempt to control the motion of fluids have been extensively explored in the past. These methods can be passive or active, or both (Gad-el-Hak 2000). Active flow control (AFC) methods, however, are much more efficient. AFCs can adapt to the constantly changing conditions by introducing small amounts of energy locally to achieve non-local changes in the flow field with large performance gains (Amitay *et al* 1998, Gad-el-Hak 2000, Kral *et al* 1997, Smith and Glezer 1998). McLean *et al* evaluated different AFC concepts, and candidate applications were considered for civil jet transports (McLean *et al* 1999). The simplification of conventional high lift systems by AFC was identified as a prime candidate, possibly providing 0.3% airplane cost reduction, up to 2% weight reduction and about 3% cruise drag reduction. In spite of all the advantages, using active flow control devices usually adds complexity in design, and increases manufacturing and operation cost, which prevents their use. For this reason, many researchers have focused on designing better active flow control devices that are easy to manufacture, are small in size and require little power to operate. One of the devices that fulfill all of these qualities is called synthetic jets.

Synthetic jets consist of a cavity with an oscillating diaphragm. When the diaphragm oscillates air is pushed out of an orifice, forming a jet (Smith 1999). A schematic of the jet formation is shown in figure 1, where one side of the orifice is called the active cavity, and the other side is the passive cavity, as indicated. The interaction of the jets with an external flow leads to the formation of closed recirculating flow regimes near the surface which act as 'virtual surfaces', causing an apparent modification of the flow boundary (Amitay *et al* 1997).

The oscillating diaphragm used in the synthetic jet cavity is usually driven using electrical or mechanical power. In the past, researchers have used compressed air or regulated blowers as a means of supplying steady or oscillating flow (Seifert *et al* 1993, 1996). This adds to the complexity and weight of the system. When driven with an AC signal, piezoelectric disks oscillate in the same manner as a piston or a shaker, and they also require reduced number of moving parts which are prone to failure. Because of these advantages, several investigators have adopted piezoelectric disks in synthetic jets to attempt to make the systems lighter, increase efficiency and save resources (Crook *et al* 1999, Rathnasingham and Breuer 1997a, 1997b, Smith and Glezer 1998). Although these piezoelectric disks have been successful in generating high velocities capable of altering the flow fields, the devices operate at high frequencies, consequently requiring high amounts of power. Also it was found that, after a time, the PZT disk would start to delaminate and/or the output of the device would drop and the resonant frequency would change.

In the current study, piezoelectric composites are used as active diaphragms in the jet cavity. In addition to active piezoelectric layers, they are reinforced with layers of metal or other stronger materials that also increase actuator durability. These composites, besides being lightweight, have the ability to produce microscale displacements and provide a wide bandwidth response. Such advantages make them suitable for flow control purposes, as demonstrated by Mossi *et al* (Mossi and Bryant 2003, 2004, Mossi *et al* 2005a).

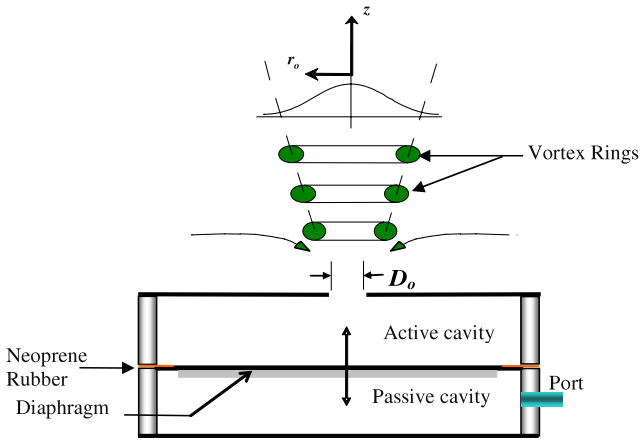

Figure 1. Synthetic jet cavity schematic.

Synthetic jets have potential applications ranging from jet vectoring (Smith and Glezer 1997), mixing enhancement (Chen *et al* 1999, Davis and Glezer 1999), to active control of separation and turbulence in boundary layers (Amitay *et al* 1997, 1998, Crook *et al* 1999). Development of practical applications using this technology requires extensive research into their performance under various conditions, since performance depends on the geometry of the jet cavity, the oscillating diaphragm used, and electrical driving conditions amongst other factors.

Although experimental investigations are capable of providing insight into the operation of a synthetic jet, a parametric study of the flow configuration through experiments is a time consuming and expensive proposition. Design of experiments (DoE) theory provides an alternate and efficient approach to accomplish the same goals. Since the performance of the jet is dependent on a number of factors, such statistical tools give a direction towards the relevant areas of synthetic jet research. Regression models can also be used in the modeling of response surfaces to optimize the performance of piezoelectric composites as synthetic jets. In this study such a statistical approach is adopted to study synthetic jet actuators formed with three unique piezoelectric composite diaphragms, Bimorph, Thunder® and Lipca. The experimental setup and results are discussed in sections 2 and 3.

2. Experimental setup

The piezoelectric diaphragms used in this study include Bimorph, Thunder® and Lipca. This section gives a detailed description of the construction of these piezoelectric composites. Also, the synthetic jet cavity and the various instruments used for the velocity and pressure measurements are described.

2.1. Bimorph

Bimorphs consist of two thin ceramic sheets bonded together with their poling directions opposed and normal to the

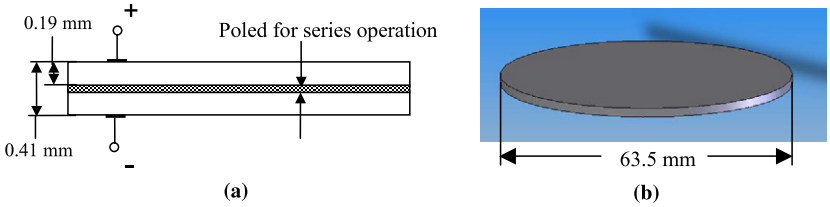

Figure 2. Bimorph: (a) schematic of its operation, (b) overall dimensions.

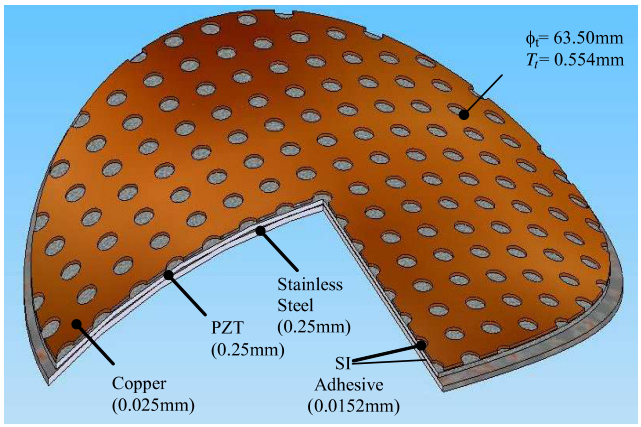

Figure 3. Thunder® (T_t refers to the active layer thickness only).

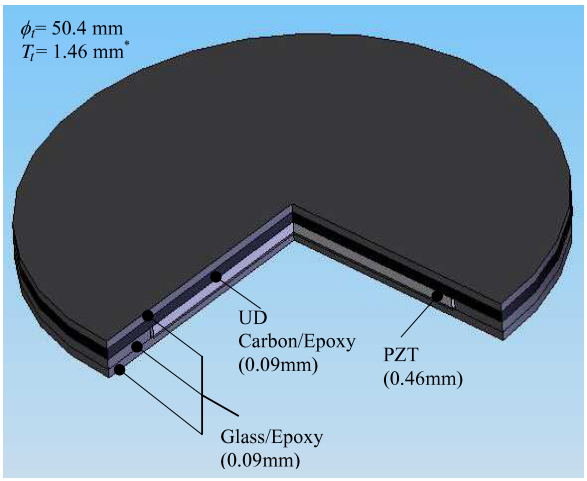

Figure 4. Lipca (T_t refers to the active layer thickness only).

interface, as shown in figure 2(a). When an electric field is applied to a Bimorph, one of the plates expands while the other contracts. This mechanism creates a bending mode that mimics piston-like displacement. Bimorphs are capable of generating large bending displacements of several hundred micrometers on center or edge, but the response time (1 ms) and the generative force (1.0 N) are low (Dogan *et al* 2001). In the current study, the Bimorph used is model T216-A4NO-573X manufactured by Piezoelectric Systems Inc. It consists of two nickel electroded PZT 5A disks with diameters of 63.5 mm and a total thickness of 0.41 mm. They have a capacitance of 130 nF at 1 kHz and have been shown to produce displacements up to 0.3 mm at low frequencies (Mossi *et al* 2005a). A schematic of the disk alignment along with the final shape is shown in figures 2(a) and (b).

2.2. *Thunder®*

Thin layer composite Unimorph ferroelectric Driver and Sensor (Thunder®) was developed at NASA Langley Research Center. It is a diaphragm that exploits the coefficients of thermal expansion mismatch between materials (Dausch and Wise 1998, Haertling 1994, Mossi *et al* 1998, Wise 1998). The significant advantage that Thunder® diaphragms have over other Unimorph benders is their extremely rugged construction. This allows them to be readily used in commercial applications, such as synthetic jets (Smith 1999). The mechanical advantage of the Thunder® design is due to the increased flexibility of the device and the radial expansion created by the pairing of preselected thermally mismatched materials (Hellbaum *et al* 1997).

Thunder® diaphragms can be fabricated in virtually any size and thickness (Mossi *et al* 1998). A circular device manufactured by Face International Inc. is used in the present study. It is composed of three main layers, with two additional thin bondlines: a top chemically etched copper with perforations of approximately 2 mm to change its stiffness, 0.0254 mm thick, a middle piezoelectric layer of thickness 0.254 mm, and a bottom 0.254 mm thick layer of stainless steel. The copper and ceramic layers have diameters of 63.5 mm and the steel layer 68.58 mm, leaving a circular tab along the edge of 2.54 mm. This additional tab is included in the design to facilitate clamping of the device. The layers are laminated with a high-temperature polyimide adhesive (Bryant 1996) through a layering high-temperature bonding process (Mossi *et al* 1998). The resulting actuator is saddle shaped with a capacitance of 110 nF at 1 kHz, as shown in figure 3. The piezoelectric ceramic used in both these diaphragms is a soft PZT type 5A. Thunder® exhibits its highest displacement at the center of the dome, and the displacement decreases drastically towards the edge of the actuator (Mossi and Bryant 2004). The maximum center displacement measured is approximately 0.06 mm with a sawtooth signal at 5 Hz (Mossi *et al* 2005b).

2.3. *Lipca*

Lightweight piezo-composite curved actuator (Lipca) is a powerful diaphragm that can be used for adaptive structure applications. Lipca is manufactured by co-curing layers at 177 °C: glass/epoxy layer, unidirectional carbon/epoxy

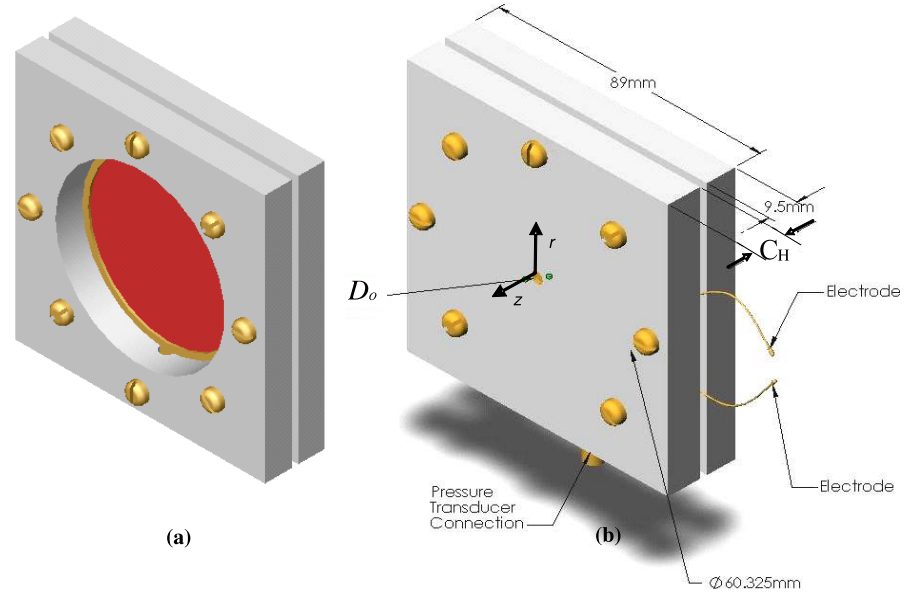

Figure 5. Synthetic jet cavity: (a) clamped actuator, (b) final assembly.

layer, and ceramic layer (Park *et al* 2002, Yoon *et al* 2002). Differences in the coefficient of thermal expansion (CTE) of the layers result in the Lipca's post cure curvature. Based on the arrangement of the layers, the curvature and the displacement vary (Yoon *et al* 2003a). The Lipca shown in figure 4 is made by Konkuk University, South Korea. It has a high CTE top layer of glass/epoxy with diameter 66.0 mm and thickness 0.09 mm, a near zero CTE unidirectional carbon/epoxy layer with 66.0 mm × 1.0 mm dimensions, a layer of PZT 5A ceramic 50.0 mm × 0.46 mm, and another glass/epoxy layer with the same dimensions in the bottom, as shown in figure 4.

The circular Lipca is not as curved as the circular Thunder® but produces higher center displacement of approximately 0.075 mm with a sawtooth driving signal at 25 Hz (Mane 2005). The difference in curvature is due to the fact that the processing temperature used for the Lipca is less than that utilized when manufacturing Thunder® (Yoon *et al* 2003b). The capacitance is approximately the same as that of the Thunder®, 100 nF.

2.4. Synthetic jet cavity

The synthetic jet cavity is constructed of two 88 mm by 88 mm Plexiglas™ pieces. The plastic pieces have a 60.5 mm circular aperture in the center. A 5 mm wide and 1 mm deep groove is machined along the perimeter of the aperture. The diaphragms are placed in between the two grooves reinforced with neoprene rubber on both sides to provide both a cushion and a seal, as shown in figure 5(a). The plastic pieces are sealed together along with a 1.6 mm thick covering plate that provides an axisymmetric orifice in the center. Seven 4 mm screws with washers are used to clamp the cavity, while one screw hole is left empty to serve as a port for the actuator electrical leads and any additional attachments to the cavity. Equal torque of 424 N mm is applied on each screw using a torque screwdriver to ensure constant pressure along the perimeter of the actuator, as shown in figure 5(b).

The cavity setup utilized allows variations in cavity height and orifice dimensions. The two cavities have overall dimensions of 88.0 mm × 88.0 mm × 19.1 mm and 88.0 mm × 88.0 mm × 11.0 mm, which correspond to cavity heights of 9.55 mm and 5.5 mm respectively. This cavity height, C_H, is measured from the diaphragm to the orifice exit. Two cover plates with circular orifices with approximate diameters, D_o, of 2.0 and 3.67 mm are used.

2.5. Instrumentation and measurements

The driving signal is applied at high voltages and varying frequencies for each device. This signal is applied using a signal generator, a Hewlett Packard model HP33120, connected to an amplifier, TREK model PZD700. The velocity and voltage signals are monitored and recorded using an oscilloscope, LeCroy model 350L, and a National Instruments data acquisition system, as shown in figure 6. The amplitude and frequency of the applied signal were kept below their allowable maximums in order to prevent electrical and mechanical failure of the diaphragms. Specifically, the field for each diaphragm was kept at a maximum of 750 V mm^{-1}. Two driving signals, sine and sawtooth, are used with all experiments.

The velocity is measured in quiescent air at a fixed distance of 2 mm in the z direction for each actuator. To obtain profiles along the length of the orifice, the velocity is measured at various locations along the orifice. To study the effects of frequency on the jet, the velocity is measured at several frequencies up to 100 Hz. These experiments are conducted on four synthetic jet cavity configurations. The differences in the cavities are the cavity height and the orifice diameter.

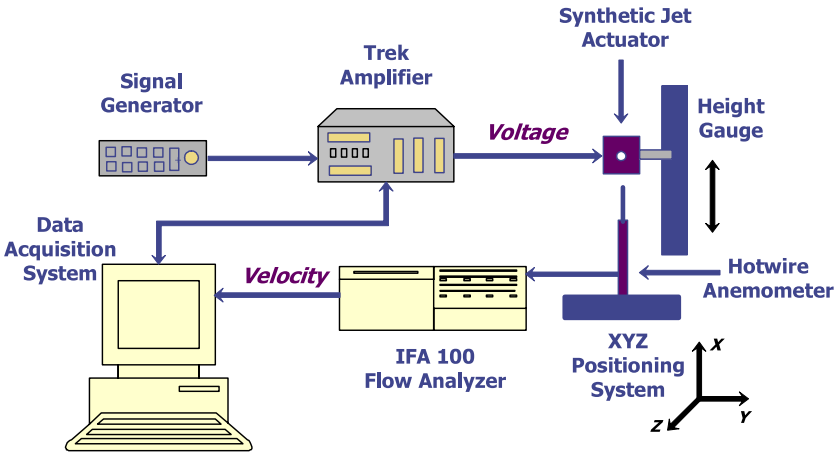

Figure 6. Synthetic jet actuator experimental setup schematic.

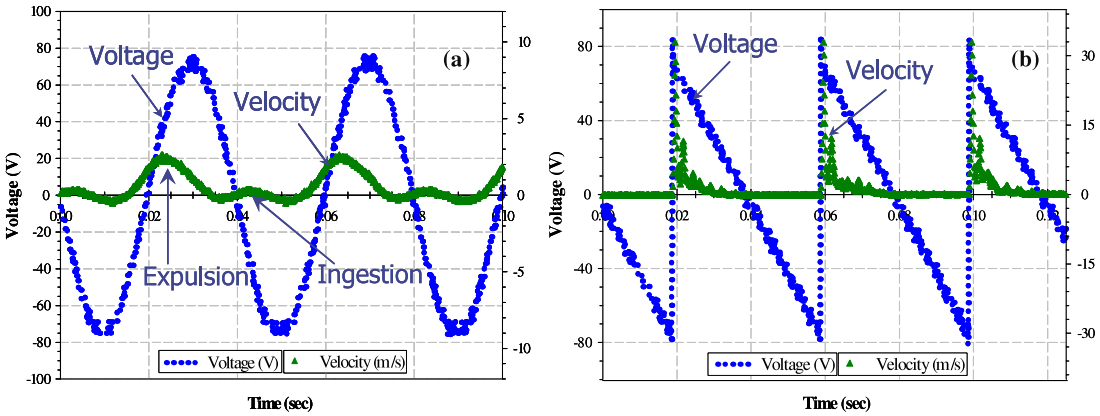

Figure 7. Typical velocity curve: (a) sine driving voltage for a Bimorph at 100 Hz and 150 V_{pp}; (b) sawtooth driving voltage for a Lipca at 25 Hz and 350 V_{pp}.

3. Experimental results

Previous studies on synthetic jets have used the sine wave as the driving input signal. A sine wave as the driving input requires relatively high frequencies matching the actuators' resonance frequency to enable the formation of a synthetic jet with significant velocity magnitude (Gallas *et al* 2002). High frequencies, however, consume more power and also physically limit the oscillation amplitude of the piezoelectric diaphragm. A sawtooth signal provides a desirable alternative to these limitations. A typical velocity curve formed with a sine wave is shown in figure 7(a). Two jets are observed, with the second jet smaller in magnitude. The first jet (larger jet) follows the leading edge of the input signal and the second jet (smaller jet) follows the trailing edge. The larger jet is believed to occur during the expulsion cycle, while the smaller jet is believed to occur during the ingestion cycle. Previous studies on the synthetic jet flow fields have indicated that during the ingestion cycle the flow reenters the cavity from the sides of the orifice (Smith and Glezer 1998). Thus the second jet may be due to the nonparallel direction of the flow, relative to the hotwire, entering the cavity. At lower frequencies, only one jet is formed, indicating that at lower frequencies the flow during the ingestion cycle is nearly parallel to the hotwire anemometer and hence cannot be detected. In the case of the sawtooth signal a single velocity jet is formed. As shown in figure 7(b), the jet follows the leading edge of the input signal, with series of smaller jets immediately following the first jet.

The velocity profiles of maximum velocity at the orifice exits of the different cavities tested are also measured. A typical result is shown in figures 8(a) and (b) for a sine wave and a sawtooth respectively. These peak velocity values are used in the statistical analysis presented in the following sections.

4. Statistical analyses and results

In this section a detailed description of the analysis of the experimental results is described. In these experiments one or more variable or factors are deliberately changed in order to observe the effect on an objective function or response variable. Initially five factors are considered, such that screening experiments are used to determine if these factors have little or no effect on the response. The factors identified as important are then investigated more thoroughly in a subset experiment with four factors.

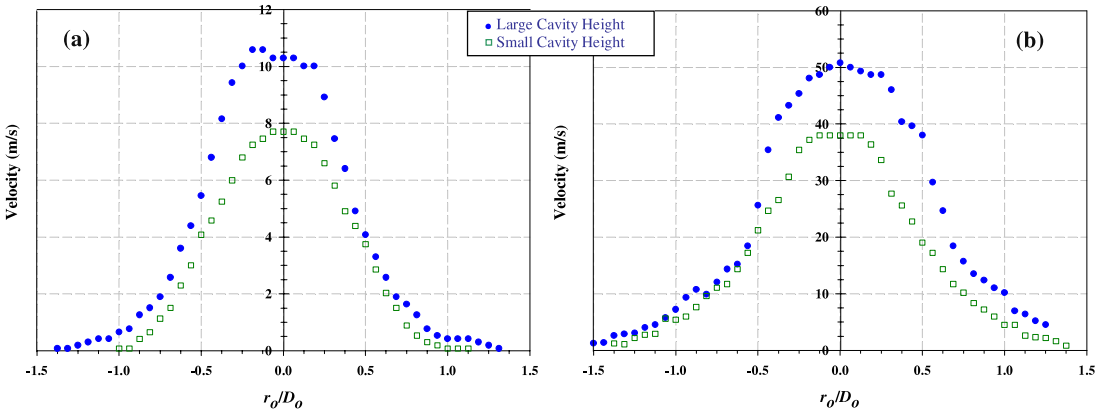

Figure 8. Typical velocity profiles: (a) for a sine waveform, (b) for a sawtooth waveform.

Table 1. Fractional factorial experimental design.

Run no. j	Factors (X_i)					Response$_j$ Y_j
	F_z	E	f	D_o	C_H	
1	−1	−1	−1	−1	+1	y_1
2	1	−1	−1	−1	−1	y_2
3	−1	+1	−1	−1	−1	y_3
4	+1	+1	−1	−1	+1	y_4
5	−1	−1	1	−1	−1	y_5
6	+1	−1	+1	−1	+1	y_6
7	−1	+1	+1	−1	+1	y_7
8	+1	+1	+1	−1	−1	y_8
9	−1	−1	−1	+1	−1	y_9
10	+1	−1	−1	+1	+1	y_{10}
11	−1	+1	−1	+1	+1	y_{11}
12	+1	+1	−1	+1	−1	y_{12}
13	−1	−1	+1	+1	+1	y_{13}
14	+1	−1	+1	+1	−1	y_{14}
15	−1	+1	+1	+1	−1	y_{15}
16	+1	+1	+1	+1	+1	y_{16}

For the first stage, several discrete or continuous input factors that can be controlled are chosen. In the current study, five factors were considered for each actuator: driving waveform, voltage, frequency, cavity height, and orifice size. The peak velocity of the jet is used as the response variable. A two-level design is chosen due to the large number of factors involved. In a two-factor experimental design each factor has two levels. These levels, 'low' and 'high', are denoted by '−' and '+' respectively. The high and low level values differ for each diaphragm. A full factorial design requires $2^5 = 32$ runs without center points or repetitions. Instead, a fractional factorial design, 2_V^{5-1}, was considered, requiring a total of 16 observations. The resolution of this design is a V which means that no main effects are confounded with any two-factor interactions or three-factor interactions; main effects are confounded with four factor interactions. A *fractional factorial design matrix* with five factors and 16 runs is shown in table 1.

The most common models utilized to fit experimental data take either a linear form or a quadratic form. In this case only linear models are considered, and interactions are neglected. In order to consider higher order interactions, replications and a higher resolution experimental design are needed. The empirical model is of the form shown in equation (1).

$$Y = \mu + \sum_{i=0}^{n} \beta_i X_i + \cdots + \varepsilon, \tag{1}$$

where $i = 1, 2, \ldots, n$, n being the number of factors. Here, Y is the response for given levels of the main effects X_i. The constant μ represents the sample mean of the response; the β are parameters whose values are determined, and they represent the coefficients for the considered factors, and ε is the experimental error. Statistical results are used to assess the validity and influence of the particular effect on the response. From the entries in table 1 the average effect sizes for each factor can be calculated.

Factor distributions for the devices are shown in table 2. As stated earlier, all factors have the same levels except the voltage, which varies due to the properties of the devices. However, the electric field is approximately 750 V mm^{-1} for each device.

4.1. Bimorph

The factor high and low levels for the Bimorph diaphragm are shown in table 2. The regression analysis discussed in the previous section is conducted for this device, as shown in table 3. The first part of the table shows a summary output of the regression. The R-square value is the relative predictive power of a model. The model shown has an R-square value of 0.97 and an adjusted R-square of 0.96, indicating that 97% of the data can be predicted using the model. The adjusted R-square value is a better estimate of the model as it accounts for the size of the model as well. This is unlike the R-square value, which increases as the number of factors increase even though they might not have an effect on the experiment (Montgomery 2005).

Following the summary is the analysis of variances (ANOVA). The ANOVA is sometimes called the F-test, and it helps determine the validity of the experimental design by testing the difference between two or more groups. When the F-value is larger than the *significance* F-value, the experiment design is considered to be valid, indicating that at least one of

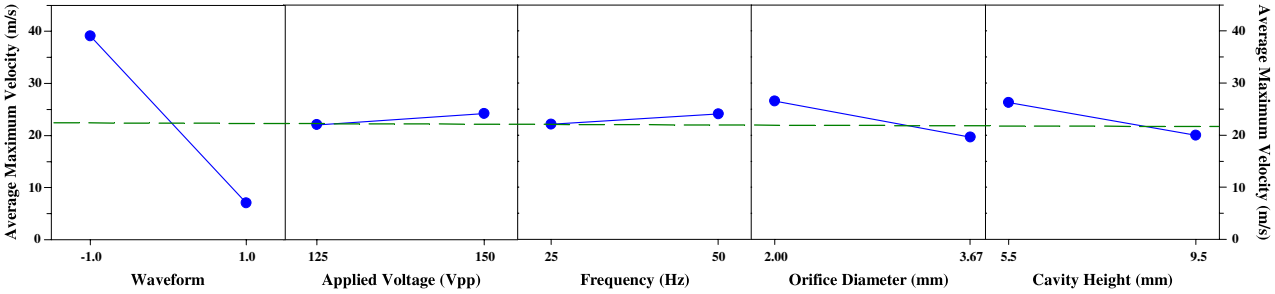

Figure 9. Average response sizes for a Bimorph diaphragm.

Table 2. Factor distribution for all devices.

Factors	Symbols	Low level (−1)	High level (+1)	Units	Types
Driving waveform	F_z	Sawtooth (−1)	Sine (+1)	None	Discrete
Applied voltage	E	125 (−1) 250 (−1) 200 (−1)	150 (+1) 400 (+1) 350 (+1)	V_{pp} (Bimorph) V_{pp} (Thunder) V_{pp} (Lipca)	Continuous
Frequency	f	25 (−1)	50 (+1)	Hz	Continuous
Orifice size	D_o	2 (−1)	3.67 (+1)	mm	Continuous
Cavity height	C_H	5.5 (−1)	9.5 (+1)	mm	Continuous

Table 3. Regression analysis for a Bimorph device.

Multiple R	0.98
R-square	0.97
Adjusted R-square	0.96
Standard error	3.38
Observations	16

	Coeffs	Std. error	t stat	p-value	Low 95%	Up 95%	Low 95%	Up 95%
Inter.	23.08	0.85	27.29	3.62×10^{-12}	21.24	24.92	21.24	24.92
F_z	−16.05	0.85	−18.97	2.58×10^{-10}	−17.89	−14.21	−17.89	−14.21
D_o	−3.47	0.85	−4.10	1.48×10^{-3}	−5.31	−1.62	−5.31	−1.62
C_H	−3.13	0.85	−3.71	3.01×10^{-3}	−4.98	−1.29	−4.98	−1.29

the factors has an effect on the response variable. The F-value shown in table 3 is computed from the mean-square values, and *significance* F-value is selected from the F-distribution tables based on the size of the sample, the number of factors, and the significance level selected, which is 95% in this case. As the F-value is larger than the *significance* F-value as seen in table 3, the experiment design is considered to be valid, and further analysis of the design can continue.

The ANOVA only shows that the experimental design as a whole is valid, but all the factors considered in the design may not be relevant. The analysis following the ANOVA helps in determining the importance of all factors. The factors are analyzed on the basis of the corresponding *p-value* generated in the table. The *p-value* or calculated probability is the estimated probability of rejecting the null hypothesis of a study question when that hypothesis is true. If the *p-value* is less than the chosen significance level then the null hypothesis is rejected. The choice of significance level at which the hypothesis is rejected is arbitrary. In the current study, the null hypothesis is that none of the factors considered in the study are significant enough such that they may affect the jet velocity. The alternate hypothesis is that one or more factors are significant, and to identify these factors the corresponding *p-values* are considered. Conventionally for this analysis the 5% (less than 1 in 20 chance of being wrong) levels or the 95% confidence internal mark has be chosen such that the *p-value* has to be less than 0.05 (Montgomery 2005).

The p-values for F_z, D_o and C_H are found to be below the 0.05 mark at 2.58×10^{-10}, 1.48×10^{-3} and 3.00×10^{-3} respectively. For the fractional factorial design of table 1 the other two factors, E and f, did not appear to be significant. This does not indicate that these factors can be ignored completely. Interaction with main effects may be present, but as the focus is only on linear models any additional effects are not taken into account in this study. From these results, a model is obtained as shown in equation (2) such that Y is the velocity in m s^{-1}. This equation shows that F_z, D_o and C_H, the main effects, can be linearly related to each other by equation (2).

$$Y = 23.08 - 16.05F_z - 3.47D_o - 3.13C_H. \quad (2)$$

Plots of all the effects showing the average responses are shown in figure 9. The main effects, F_Z, D_o, and C_H, have a large slope, as seen in the plots, and the remaining factors have a very small slope, indicating that they do not have a significant effect on the jet velocity.

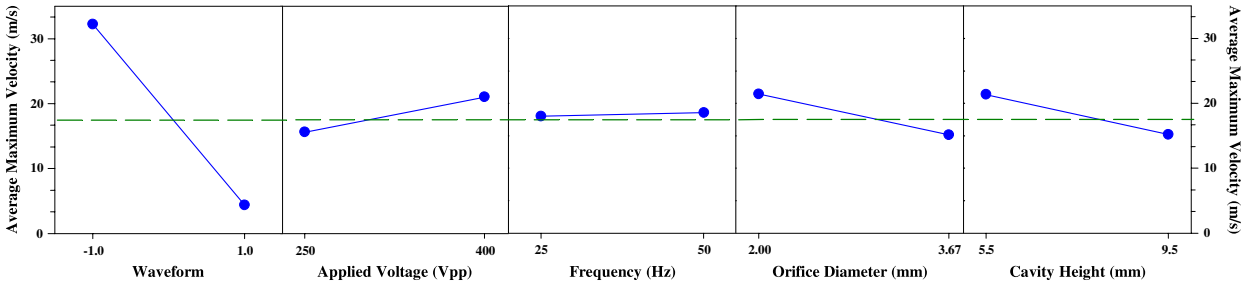

Figure 10. Average response sizes for a Thunder diaphragm.

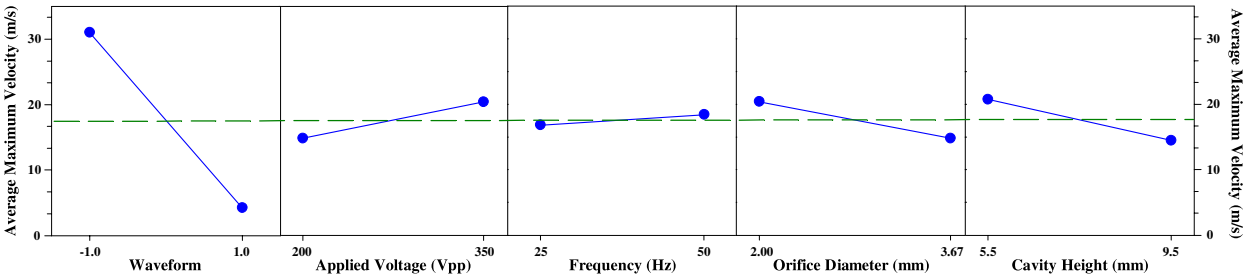

Figure 11. Average response sizes for a Lipca diaphragm.

Table 4. Regression analysis for a Thunder® device.

Multiple R	0.97
R-square	0.94
Adjusted R-square	0.92
Standard error	4.55
Observations	16

	Coeffs	Std. error	t stat	p-value	Low 95%	Up 95%	Low 95%	Up 95%
Inter.	18.29	1.14	16.08	5.46×10^{-9}	15.78	20.79	15.78	20.79
F_z	−13.92	1.14	−12.24	9.50×10^{-8}	−16.42	−11.41	−16.42	−11.41
E	2.70	1.14	2.37	0.037	0.19	5.20	0.19	5.20
D_o	−3.16	1.14	−2.78	0.018	−5.66	−0.65	−5.66	−0.65
C_H	−3.07	1.14	−2.70	0.021	−5.57	−0.57	−5.57	−0.57

4.2. Thunder

A similar process used for the Bimorph is repeated for the Thunder® with the same factors. The only difference in this case is the factor levels for applied voltage (E). As shown in table 2 the voltage levels of 250 V_{pp} (low level, −1) and 400 V_{pp} (high level, 1) are used for the Thunder diaphragm; however, the response variable, maximum jet velocity, is the same. The 2^{5-1} fractional factorial experimental design from table 1 is used here as well. All the 16 runs with different level combinations for each factor are listed. A regression analysis with 95% confidence interval is shown in table 4. The regression has an R-square value of 0.94 and an adjusted R-square value of 0.92. Only one factor, frequency f, is eliminated as its *p-value*, 0.807, is above the critical value of 0.05 for a 95% confidence interval analysis. This meant that the remaining four factors, F_Z, E, D_o and C_H, having *p-value* 9.50×10^{-8}, 0.037, 0.018 and 0.021, respectively had main effects. Frequency was not a main effect, but it could have an interaction effect which cannot be neglected.

Using the coefficient values calculated in the regression a linear model fit is obtained, shown by equation (3), where Y is the velocity in m s^{-1}. The average response plots are shown in figure 10.

$$Y = 18.287 - 13.92F_z + 2.70E - 3.16D_o - 3.07C_H. \quad (3)$$

4.3. Lipca

The procedure used in case of the Bimorph and Thunder® devices is repeated for the Lipca as well. The levels for each factor (table 2) are chosen based on the characteristics of the actuator. Except for the driving waveform factor all the factors are continuous. Maximum jet velocity is the response variable. The same table 1 design matrix used for the Bimorph and Thunder is used here too. The 95% confidence interval regression analysis shown in table 5 helps in identifying the main effects. Since frequency, f, has a *p-value* of 0.48, which is above 0.05, it is not considered as one of the main effects. The other four factors have valid *p-values*; thus they are considered as main effects. The *p-values* of the selected

Table 5. Regression analysis for a Lipca device.

Multiple R	0.97							
R-square	0.94							
Adjusted R-square	0.92							
Standard error	4.32							
Observations	16							
	Coeffs	Std. Error	t stat	p-value	Low 95%	Up 95%	Low 95%	Up 95%
Inter.	17.62	1.08	16.31	4.72×10^{-9}	15.24	19.99	15.24	19.99
F_z	−13.41	1.08	−12.41	8.24×10^{-8}	−15.78	−11.03	−15.78	−11.03
E	2.79	1.08	2.58	0.025	0.41	5.17	0.41	5.17
D_o	−2.78	1.08	−2.57	0.026	−5.16	−0.40	−5.16	−0.40
C_H	−3.12	1.08	−2.89	0.015	−5.50	−0.74	−5.50	−0.74

Table 6. Fractional factorial design, 2_V^{4-1}.

F_z	E	f	P_B
−1	−1	−1	−1
1	−1	−1	1
−1	1	−1	1
1	1	−1	−1
−1	−1	1	1
1	−1	1	−1
−1	1	1	−1
1	1	1	1

factors are 8.24×10^{-8} for F_Z, 0.025 for E, 0.026 for D_o and 0.015 for C_H. The regression has an R-square value of 0.94 and an adjusted R-square value of 0.92.

Using the coefficients obtained from the regression analysis a model fit is possible, as given by equation (4). The factors included in the equation are considered as main effects, with Y as the velocity of the jet in m s^{-1}. Figure 11 shows the slope of the different effects, confirming again the results obtained in the statistical regression.

$$Y = 17.6170 - 13.41F_z + 2.79E - 2.78D_o - 3.12C_H. \quad (4)$$

In the three diaphragms tested the frequency factor was found to have minimal effect on the synthetic jet velocity, while the driving signal and cavity dimensions had significant effects. All other factors were significant.

4.4. Back pressure effects

Besides the factors considered in this project the study can be expanded to include a number of additional factors, such as the cavity shape, the orifice plate thickness, the orifice shape, the size of the diaphragm, etc. One factor of interest that is not included in the previous design is the *back pressure* that a synthetic jet actuator may experience when mounted in a wing or a body in flight. To explore the significance of this effect, a second set of experiments is designed where the passive cavity is pressurized. This is accomplished by applying compressed air from a regulated supply through the port shown in figures 1 and 5(b), labeled pressure transducer connection. Through this port, a pressure regulator controls the pressure in the passive cavity to desired levels. Again the velocities are measured and profiles mapped with different pressure levels in the passive cavity. A two-level screening experiment is considered with only four factors using a V resolution fractional factorial design: waveform, F_z, field, E, frequency, f, and back pressure, P_B. The factor 'high' and 'low' levels are identical to the previous regressions as listed in table 2, with the addition of P_B. The P_B low (−1) and high (1) levels are set at 0 and 17.24 kPa respectively. In this regression, main effects are not confounded with any two-factor interactions, but main effects are confounded with three-factor interactions. This design, 2_V^{4-1}, is shown in table 6, with the response variable again peak velocity measured at the orifice exit. For this design a cavity is randomly selected, thus reducing the number of factors in the design to 4, keeping the cavity dimensions ($D_o = 3.67$ mm and $C_H = 9.55$ mm) constant.

The average response sizes for the smaller design are shown in figure 12. This design also confirms the waveform as the main effect for every device, while the other effects are not clear. By performing a series of regressions to identify the significance of each factor for the first actuator, the Bimorph, the waveform effect becomes evident, as shown in table 7. However, the back pressure effect is not clearly statistically significant, with a *p-value* close to the confidence level assigned, 95%. This fact coupled with the results showed in figure 12(a) indicates that more data are needed to obtain a statistically significant result in the analysis of this diaphragm's performance as a synthetic jet device since two-factor interactions may be present. Adding center points to this design or changing the resolution of the design may provide more insight on the relevance of the considered factors.

In the case of the Thunder diaphragm, statistically significant interactions among the factors tested were identified. Waveform and pressure interaction as well as waveform and field interactions are statistically significant, and are hence included in the design. Other two-factor interactions tested are not statistically significant, and are hence eliminated from this final design. These results, shown in table 8, confirm the results shown in figure 12(b), where all the factors tested seemed to have an effect on the response. The *p-values* obtained for this regression were all less than 0.05 and the *R-value* was 99%.

Using the Thunder regression, figures 13(a) and (b) can be constructed. These figures show the direction of steepest ascent. In figure 13(a) an increase in frequency and voltage show the line of steepest ascent occurs at a slope of approximately 0.7. In figure 13(b), again an increase

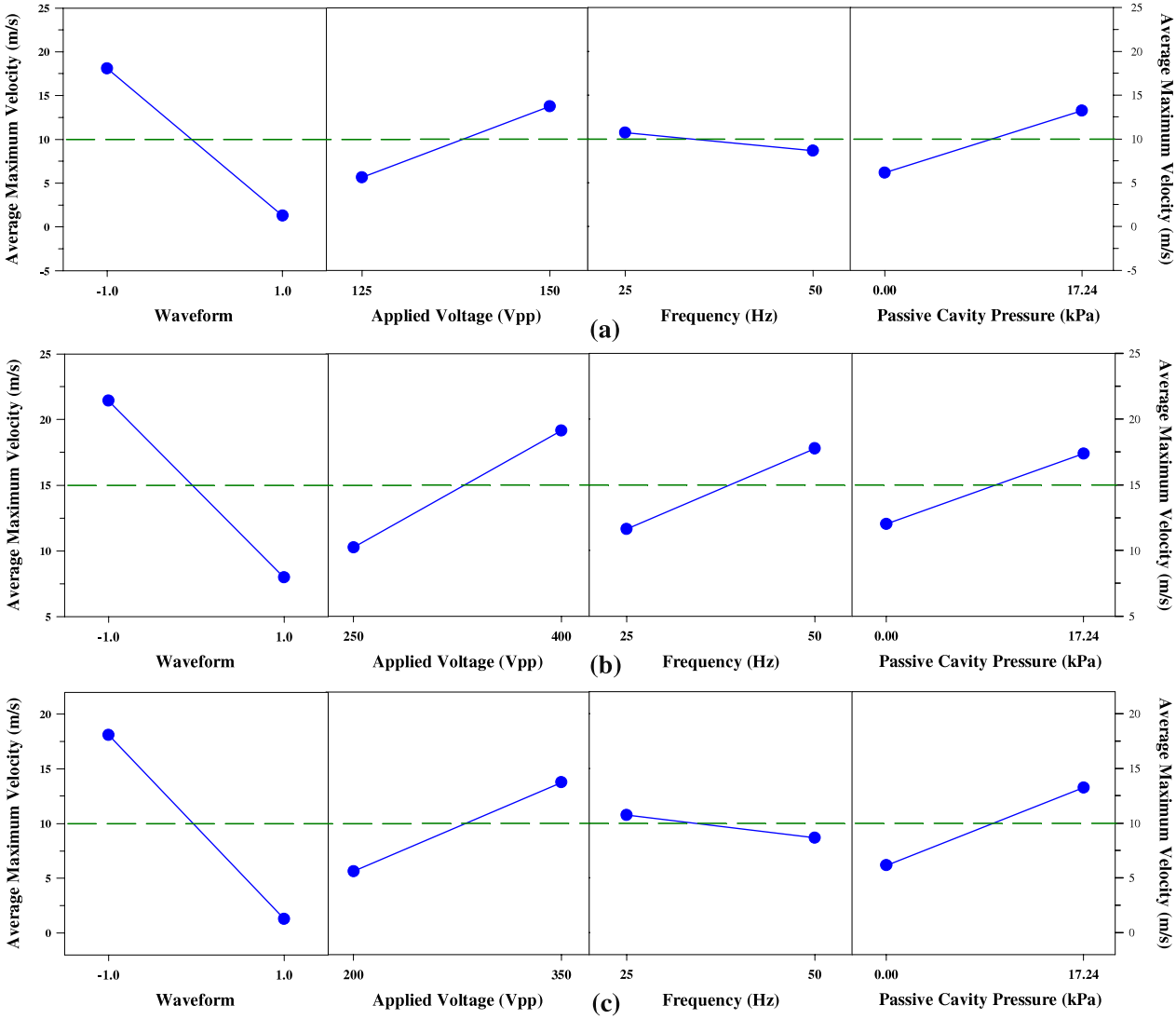

Figure 12. Average response sizes: (a) Bimorph, (b) Thunder and (c) Lipca.

Table 7. Final estimate of the significance of the factors tested for a Bimorph.

Multiple R	0.927							
R-square	0.859							
Adjusted R-square	0.804							
Standard error	6.017							
Observations	8							
	Coeffs	Std. error	t stat	p-value	Low 95%	Up 95%	Low 95%	Up 95%
Inter.	12.62	2.127	5.932	0.0019	7.151	18.09	7.152	18.00
F_z	−10.65	2.127	−5.005	0.0041	−16.116	−5.179	−16.117	−5.179
P_B	−5.06	2.127	−2.380	0.0632	−10.532	0.406	−10.532	0.406

in frequency and back pressure shows that the slope is 1.1. This indicates that to maximize velocity the path of steepest ascent is through increasing pressure. The practical part of this approach is the limit that each diaphragm can withstand before rupture. This fact can be used in the optimization of the performance of a synthetic jet under specific conditions.

Similar to Bimorph, the regression analysis for the Lipca device shows the waveform effect to be the most significant. Although back pressure and frequency effects are eliminated from the analysis, a definite conclusion cannot be reached for the effect of electric field, as seen in table 9. The data available are not sufficient to obtain a satisfactory regression model. However, changing the design parameters and adding center points can provide more insight into these results, but is not a part of this study.

Considering the magnitudes of the jet velocities measured with each device the Bimorph was seen to produce the highest range of velocities and the Thunder® and Lipca produced

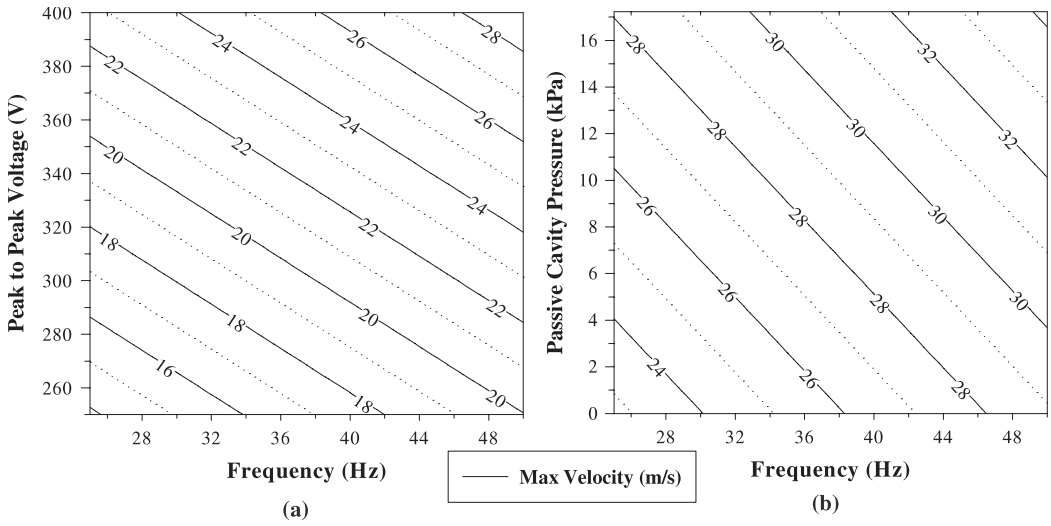

Figure 13. Contour plots of maximum velocity for the Thunder device: (a) E versus f, (b) P_B versus f.

Table 8. Final estimates of the significance of the factors tested for a Thunder.

Multiple R	0.999
R-square	0.999
Adjusted R-square	0.999
Standard error	0.191
Observations	8

	Coeffs	Std. err	t stat	p-value	Low 95%	Up 95%	Low 95%	Up 95%
Inter.	14.69	0.0676	217.3	0.0029	13.83	15.55	13.83	15.55
F_z	−6.730	0.0676	−99.5	0.0064	−7.59	−5.87	−7.58	−5.87
E	4.45	0.0676	65.8	0.0097	3.5908	5.31	3.59	5.31
f	3.06	0.0676	45.31	0.0141	2.2046	3.92	2.21	3.92
P_B	2.67	0.0676	39.46	0.0161	1.8096	3.53	1.81	3.53
$F_z P_B$	3.59	0.0676	53.09	0.0119	2.7309	4.45	2.73	4.45
$F_z E$	−0.99	0.0676	−14.69	0.0433	−1.8531	−0.13	−1.85	−0.13

Table 9. Final estimates of the significance of the factors tested for a Lipca.

Multiple R	0.826
R-square	0.682
Adjusted R-square	0.554
Standard error	6.973
Observations	8

	Coeffs	Std. error	t stat	p-value	Low 95%	Up 95%	Low 95%	Up 95%
Inter.	14.692	2.465	5.959	0.002	8.355	21.030	8.355	21.030
F_z	−6.730	2.465	−2.730	0.041	−13.068	−0.393	−13.068	−0.393
E	4.449	2.465	1.805	0.131	−1.888	10.787	−1.888	10.787

lower velocities in a similar range. All the actuators produced velocities in the range of 25–50 m s^{-1}.

5. Conclusions

Three diaphragms, Bimorph, Thunder® and Lipca, are studied as synthetic jet diaphragms. Using statistical analysis tools such as screening designs and fractional factorial models, an analysis of significance is performed on several variables with peak jet velocity as the objective function. The six factors studied are the driving signal used to excite the diaphragms, the magnitude and frequency of the signal, the volume of the cavity described by the cavity height, the size of the exit or orifice, and the pressure in the passive cavity of the jet. To study these six factors, the study is divided into two sets, one that studies the first five factors, and a smaller fractional factorial design to study the last factor, passive cavity pressure. In this manner, the relevant factors can be identified based on statistical significance.

In the first screening design the factors are evaluated at two levels each: driving signals, sine and sawtooth; voltage level, low and high; frequency, low and high; cavity height, low and high; orifice size, large and small. This stage of the analysis showed that three factors were statistically significant

in all three piezoelectric diaphragms: driving signal, orifice diameter, and cavity height. In contrast, frequency was found to be a non-significant factor in all the three diaphragms. These conclusions are limited to non-resonant conditions when back pressure is not a factor. A comparison of the regression coefficient sizes for each actuator suggests the possibility of a larger model that could include the diaphragm as a factor. A larger experimental design can then be designed in future studies.

The last factor studied was the effect of pressurizing the passive cavity in the form of a uniformly distributed load on the diaphragm. Keeping the orifice size and cavity height constant, a fractional factorial design was performed on four factors: driving signal, magnitude and frequency of the signal, and passive cavity or back pressure. In this analysis, along with the main factors, the interactions between the factors were also evaluated. Unlike the previous design, all diaphragms showed different results in this design. In case of the Thunder diaphragm, statistically significant interactions among the factors tested were identified. All main effects proved to be statistically significant along with waveform–pressure and waveform–field interactions. Although the results were conclusive for the Thunder, the data proved to be insufficient for the other two devices. For the Bimorph and Lipca devices the waveform effect was again identified as a statistically significant factor.

In summary, the applied waveform is an important factor when maximizing jet velocity, independent of the active diaphragm used in the synthetic jet actuator. In addition, frequency was not relevant in all cases within the studied limits. This study indicates that to optimize the performance of a synthetic jet, the diaphragm and driving signal should be included in any design of a piezoelectric synthetic jet.

Acknowledgment

The authors would like to thank the NASA Langley Research Center for their financial support and technical assistance through grant number NNL04AA04G.

References

Amitay M, Honohan A, Trautman M and Glezer A 1997 Modification of the aerodynamic characteristics of bluff bodies using fluidic actuators *AIAA* 97–2004

Amitay M, Smith B and Glezer A 1998 Aerodynamic flow control using synthetic jet technology *AIAA* 98–0208

Bryant R G 1996 LaRC-SI: a soluble aromatic polyimide *High Perform. Polym.* **8** 607–15

Chen Y, Liang S, Aung K, Glezer A and Jogoda J 1999 Enhanced mixing in a simulated combustor using synthetic jet actuators *AIAA Paper* 1999-0449

Crook A, Sadri A M and Wood N J 1999 The development and implementation of synthetic jets for the control of separated flow *AIAA* 99-3176

Dausch D E and Wise S A 1998 Composition effects on electromechanical degradation of RAINBOW actuators *NASA TM* 1998-206282, pp 2–3, January

Davis S A and Glezer A 1999 Mixing control of fuel jets using synthetic jet technology *AIAA Paper* 1999-0447

Dogan A, Tressler J and Newnham R E 2001 Solid-state ceramic actuator designs *AIAA J.* **39** 1354–62

Gad-el-Hak M 2000 *Flow Control: Passive, Active, and Reactive Flow Management* (Cambridge: Cambridge University Press) chapter 1

Gallas Q, Mathew J, Kasyap A, Holman R, Nishida T, Carroll B and Sheplak M 2002 Lumped element modeling of piezoelectric-driven synthetic jet actuators *40th AIAA Aerospace Sciences Mtg and Exhibit* 2002-0125

Haertling G H 1994 Chemically reduced PLZT ceramics for ultra high displacement actuators *Ferroelectrics* **154** 101–6

Hellbaum F R, Bryant R G and Fox R L 1997 Thin layer composite unimorph ferroelectric driver and sensor *US Patent Specification* 5,632,841

Kral L D, Donovan J F, Cain A B and Cary A W 1997 Numerical simulation of synthetic set actuators *28th Conf. on AIAA Fluid Dynamics* pp 97–1824

Mane P 2005 Experimental design and analysis of piezoelectric synthetic jets in Quiescent *Masters Thesis* Virginia Commonwealth University, p 116

McLean J D, Crouch J D, Stoner R C, Sakurai S, Seidel G E, Feifel W M and Rush H M 1999 Study of the application of separation control by unsteady excitation to civil transport aircraft *Technical report CR* 1999-209338, NASA

Montgomery D C 2005 *Design and Analysis of Experiments* (New York: Wiley)

Mossi K and Bryant R 2003 Piezoelectric actuators for synthetic jet applications *Proc. Mater. Res. Soc. Fall Meeting (Boston, MA, USA)* p D11.8

Mossi K and Bryant R 2004 Pre-stressed circular actuators *Am. Ceram. Soc.* **150** 445–54

Mossi K, Castro N D, Bryant R and Mane P 2005b Boundary condition effects on piezo-synthetic jets *Integr. Ferroelectr.* **71** 257–66

Mossi K, Mane P and Bryant R 2005a Velocity profiles for synthetic jets using piezoelectric circular actuators *AIAA* 2005-341

Mossi K, Selby G and Bryant R 1998 Thin-layer composite unimorph ferroelectric driver and sensor properties *Mater. Lett.* **35** 39–49

Park K H, Kim Y B, Kim Y S, Park H C and Yoon K J 2002 Experimental performance evaluation of lightweight piezo-composite curved actuators *Proc. SPIE* **4699** 315–22

Rathnasingham R and Breuer K S 1997a Coupled fluid-structural characteristics of actuators for flow control *AIAA J.* **35** 832–7

Rathnasingham R and Breuer K S 1997b System identification and active control of a turbulent boundary layer *PhD Thesis* MIT

Seifert A, Bachar T, Koss D, Shepshelovich M and Wygnanski I 1993 Oscillatory blowing: a tool to delay boundary-layer separation *AIAA J.* **31** 2052–60

Seifert A, Darabi A and Wygnanski I 1996 Delay of airfoil stall by periodic excitation *J. Aircr.* **33** 691–8

Smith B L 1999 Synthetic jets and their interaction with adjacent jets *PhD Thesis* Georgia Institute of Engineering, p 143

Smith B L and Glezer A 1997 Vectoring and small scale motions effected in free shear flows using synthetic jet actuators *AIAA* 97-0213

Smith B L and Glezer A 1998 The formation and evolution of synthetic jets *Phys. Fluids* **10** 2281–97

Wise S A 1998 Displacement properties of RAINBOW and THUNDER piezoelectric actuators *Sensors Actuators* A **69** 33–8

Yoon K J, Park K H, Park H C, Lee S K and Goo N S 2003a Analytical design model for a piezo-composite unimorph actuator and its verification using lightweight piezo-composite curved actuators *Smart Mater. Struct.* **13** 459–67

Yoon K J, Park K H, Park H C and Perraux D 2003b Thermal deformation analysis of curved actuator LIPCA with piezoceramic layer and fiber composite layers *Compos. Sci. Technol.* **63** 501–6

Yoon K J, Shin S, Park H C and Goo N S 2002 Design and manufacture of lightweight piezoceramic curved actuator *Smart Mater. Struct.* **11** 163–8